scientific reports

Check for updates

OPEN

Hepatocellular carcinoma antibodies preferably identify nitro-oxidative-DNA lesions induced by 4-Chloro-orthophenylenediamine and DEANO

Shifa Khan[1], Asif Ali[1], Mohd Sharib Warsi[1], Sana Waris[1], Ali Raza[1], Syed Amaan Ali[2], Mohd Mustafa[1], Moinuddin[1], Shahid Ali Siddiqui[3], Riaz Mahmood[4] & Safia Habib[1]✉

The widespread use of oxidative hair colouring cosmetics threatens public health. Phenylenediamine derivatives serve as the main pigment in permanent hair colours. They interact with biological macromolecules, altering their functional and structural physiology. The study aimed to investigate the effect of a typical synthetic hair dye pigment, 4-Chloro-orthophenylenediamine (4-Cl-OPD), under a nitrating environment of DEANO on the calf thymus DNA molecule. The results showed single-stranded regions, base/sugar-phosphate backbone alterations, molecular changes, and nitro-oxidative lesions. These modifications are referred to as neo-epitopes on the DNA molecule. IgGs from cancer patients with a history of permanent hair dye use were screened for the recognition of neo-epitopes on DNA molecules. Hepatocellular carcinoma IgG showed the highest binding with 56% inhibition in the competition ELISA. The immune complex formation was observed through electrophoretic mobility shift assay. In conclusion, synthetic hair dye users are likely to present with heightened immunological triggers under elevated nitric oxide levels. The study reports chronic hair dye exposure as one of the factors responsible for altering the intricacies of the DNA's microarchitectural structure and inducing neo-epitopes on the molecule. The physiological status of NO may define the susceptibility towards 4-Cl-OPD and humoral response in hair dye users. Persistent nitro-oxidative stress due to 4-Cl-OPD and NO may induce a heightened immune response against neoepitopes in the nitro-oxidatively modified DNA. Therefore, chronic hair dye exposure may be identified as a risk to human health. These findings may contribute to a better understanding and reinforcement of hair dye as one of the modifiable risk factors responsible for the pro-inflammatory carcinogenic environment.

Keywords 4-Chloro-orthophenylenediamine, DNA, Neo-epitopes, Enzyme-linked immunosorbent assay, Hepatocellular carcinoma

Recent evidence from experimental and population-based studies has indicated that various chemicals, including cosmetic hair dyes, pigments, photographic and xerox inks, etc., are the potential skin sensitizers that induce allergic reactions[1–3]. Among the mentioned commodities, hair coloring products have gained the attention of the scientific and research community. Globally, people are voluntarily exposed to these cosmetic ingredients. The preference for permanent hair color is increasing, irrespective of gender and economic status[4–6]. The concern regarding these synthetic hair colouring products also arises because the International Agency for Research on Cancer (IARC) has asserted that certain hair dyeing chemicals are mutagenic and probably could be carcinogenic in animals and the exposed human population[7,8].

Phenylenediamines (PDs) and their isomers, like para-phenylenediamine (PPD), ortho-phenylenediamine (OPD), and meta-phenylenediamine (MPD), are the most widely used precursors in synthetic oxidative hair

[1]Department of Biochemistry, Faculty of Medicine, Jawaharlal Nehru Medical College, Aligarh Muslim University, Aligarh, Uttar Pradesh 202002, India. [2]Department of Periodontics and Community Dentistry, ZA Dental College, Faculty of Medicine, Aligarh Muslim University, Aligarh, India. [3]Department of Radiation, Mahatma Gandhi Medical College and Hospital, Jaipur, Rajasthan, India. [4]Department of Biochemistry, Faculty of Life Sciences, Aligarh Muslim University, Aligarh, Uttar Pradesh 202002, India. ✉email: saf_h75@yahoo.co.in; safia.bh@amu.ac.in

dye preparations[1,9]. Upon dermal exposure, these dye precursors induce allergic reactions in rats and sensitize the immune system, stimulating effector T-cells[10,11]. The ability of PDs to activate the immune system is thought to arise from the unstable and auto-oxidative nature of these compounds[12,13]. PDs autoxidize in the presence of molecular oxygen to form self-conjugates that, on rearrangement, form a mutagenic compound known as Bandrowski's base (BB)[11]. The hair dye components and their metabolites undergo detoxification in the liver before they are cleared from the system. The detoxification process mainly involves the acetylation of their amino group[14]. However, the addition of an electrophilic group like halogen increases stability and interferes with the detoxification process[1,15,16]. Studies have reported that PPD-containing hair dyes were detected in the urine after 48 h of the dye application, and approximately 85 percent of the amount collected in 48 h was released in the first twenty-four hours[17]. White et al. 2006, found that the PPD equivalent remained in the stratum corneum for up to 3 days following a single application of about 5 min[18]. These findings and other supporting literature point toward the potential health hazards of chronic exposure to synthetic oxidative hair dyes.

4-Chloro-orthophenylenediamine (4-Cl-OPD), a halogenated synthetic derivative of OPD, is commonly used to impart a permanent dark, luscious color (https://www.tga.gov.au/resources/publication/scheduling-decisions-interim/publication-interim-decisions-amending-or-not-amending-current-poisons-standard-february-2019/31-2-chloro-p-phenylenediamine, http://delloyd.50megs.com/hazard/carcinogens.html, https://noellesalon.com/blogs/hair-color-style/avoiding-the-risks-toxic-chemicals-in-hair-dye).

This derivative can penetrate the skin and enter systemic circulation[19–21]. Studies have also reported that 4-Cl-OPD acts by producing reactive oxygen species (ROS)[22,23]. Reactive nitrogen species (RNS) and ROS are potent molecules that interact with and damage various cellular components like nucleic acids, proteins, and lipids[24–26]. It is widely documented that ROS and RNS cause oxidative, nitrosative, and nitro-oxidative DNA damage leading to carcinogenesis[27]. The appearance of 8-oxo-7,8-dihydro-2′-deoxyguanosine (8-oxo-dG) is the hallmark of oxidative damage to DNA[27,28]. Endogenously nitric oxide (NO) is produced constitutively by endogenous nitric oxide synthase (eNOS) and neuronal nitric oxide synthase (nNOS), whereas, during stress, inducible nitric oxide synthase (iNOS) contributes to the increased plasma levels of NO in the human system. Nitric oxide is a mediator of pro-inflammatory responses, and its levels are increased aberrantly during inflammation and carcinogenic transformations. Excessive production of NO is implicated in various pathological conditions like sepsis, allergies, ischemia, diabetes, and Alzheimer's disease, as well as in cancers[28–32]. NO reacts with superoxide ($O_2^{\cdot-}$) to generate the highly damaging free radical peroxynitrite ($ONOO^-$), which can interact with DNA and results in the formation of 8-oxo-dG and 8-nitro-guanine, the markers of nitro-oxidative DNA damage[28,29]. The presence of 8-nitro-guanine in DNA creates lesions on the nucleic acid molecule that results in the formation of apurinic sites and cause G: C to T: A transversions[33–36].

Detailed investigations from our lab confirmed structural, conformational alterations and the damaging action of 4-Cl-OPD on human serum albumin (HSA) and DNA[22,23,37]. Though a number of studies point towards the genotoxic and cytotoxic nature of synthetic hair dye precursors, the evidence for the association between hair dye use and cancer development stands weak[38–40]. This study, in continuation of our earlier work, tries to explore the synergistic effect of nitric oxide and 4-Cl-OPD on calf thymus DNA. The study is mainly focused on two aspects: (a) Quantification of the neo-epitopes and (b) screening the binding specificity of antibodies isolated from different groups of cancer patients with a history of permanent hair dye use ($\geq$5 years, at least a month).

Native calf thymus DNA (nCT-DNA) was treated with 4-Cl-OPD and a NO donor diethylamineNONOate sodium salt dihydrate (DEANO). The structural modifications incurred on the DNA molecule were characterized through biophysical techniques. The quantitative analysis of the free radicals involved during the interaction of NO, 4-Cl-OPD, and DNA was identified with the help of free radical scavenger assays. Direct binding and competition ELISA were used to screen and quantify the binding specificity of cancer IgG against the neo-epitopes on the DNA molecule. The antigen and antibody complex were visualized through an electrophoretic mobility assay. This research could provide an anticipated in-depth biochemical understanding of hair dye exposure to DNA and, in the future, shed light on identifying hair dye containing 4-CL-OPD as one of the factors for inflammatory carcinogenesis.

Results

Biophysical characterization of native DNA and DNA treated with NO and 4-Cl-OPD

UV–vis and fluorescence spectroscopy

The peak at 260 nm was observed for nCT-DNA and all the modified forms of DNA. A Hyperchromicity of 10.3% was observed in the case of NO-DNA. However, 4-Cl-OPD-DNA and 4-Cl-OPD-NO-DNA exhibited a significant hyperchromic change of 22.56% and 45.2%, respectively. This increase in hyperchromicity may be due to the unwinding of the duplex DNA, which results in unstacking of the nitrogenous bases. Exposure of unstacked bases to UV light results in increased absorbance. The UV profile of 4-Cl-OPD-NO-DNA showed a small peak around 400 nm, which may correspond to the formation of 8-nitroguanine, a nitrosative DNA lesion (Fig. 1A). DNA is nonfluorescent in nature. Therefore, an external chromophore, a DNA intercalator ethidium bromide (EtBr), was used to study the effect of NO and 4-Cl-OPD on the structure of the DNA molecule. A decrease in fluorescence intensity (23.9%) was seen when the DNA was treated with 4-Cl-OPD (100 μM)[22]. However, the coincubation of DNA with 4-Cl-OPD (100 μM) and DEANO (20 μM) further decreased the fluorescence to 46.08%. This decreased fluorescence could be attributed to reduced EtBr intercalation due to the DNA helix's perturbed structure. In Fig. 1B (NO-DNA), no significant fluorescence quenching was observed.

Nuclease S1 digestibility assay to detect the presence of single-stranded regions on native and DNA treated with 4-Cl-OPD and DEANO

Nuclease S1 is an endonuclease that preferentially cleaves single-stranded nucleic acids, leaving only a double-stranded form of DNA. Here, significant digestion was observed (decreased fluorescence intensity with increased

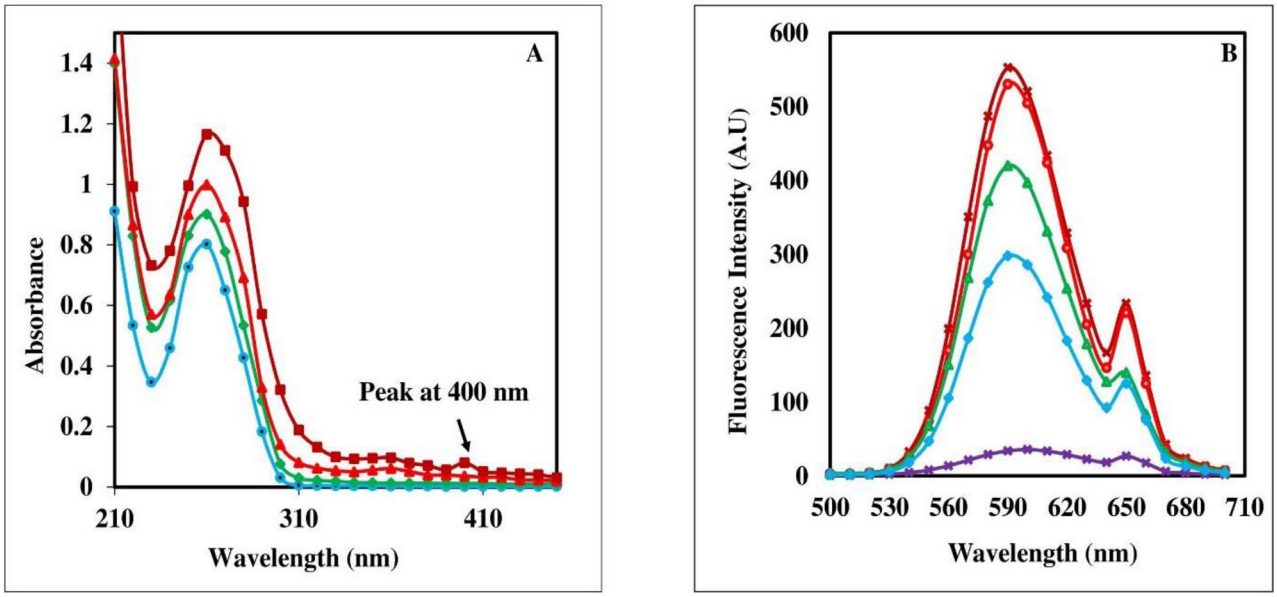

Fig. 1. (**A**) Absorbance spectra of nCT-DNA (Blue colour filled circle), nCT-DNA treated with 20 µM DEANO (NO-DNA, green colour filled diamond), nCT-DNA treated with 100 µM 4-Cl-OPD (4-Cl-OPD-DNA, red colour filled triangle) and nCT-DNA treated with 100 µM 4-Cl-OPD + 20 µM DEANO (4-Cl-OPD-NO-DNA, brown colour filled square). (**B**) Fluorescence emission spectra of native calf thymus DNA (brown cross), NO-DNA (red colour filled circle), 4-Cl-OPD-DNA (green colour filled triangle), and 4-Cl-OPD-NO-DNA (blue colour filled diamond). Ethidium bromide (2.5 µg /ml) was used as the external chromophore (violet cross). The excitation wavelength used was 325 nm.

migration of the DNA) when 4-Cl-OPD-DNA and 4-Cl-OPD-NO-DNA were treated with S1. More pronounced digestion by nuclease S1 was observed for 4-Cl-OPD-NO. However, no digestion was obtained when NO-DNA and nCT-DNA were treated with nuclease S1 (Fig. 2).

FTIR spectroscopic analysis to identify changes in the characteristic functional groups of the DNA at the molecular level

FTIR spectroscopy was used to identify changes incurred on nCT-DNA in the presence of NO, 4-Cl-OPD alone, and in combination. Also, it analyzed the nature of interactions between DNA and ligands (4-Cl-OPD and NO). The spectra were recorded in the vibration range of 800–1800 cm^{-1}. The marker absorption bands for nCT-DNA were intact and detected at 896, 1217, 1493, and 1713 cm^{-1}. These absorption bands lie in the three major regions for FTIR spectra of DNA, i.e., 1800–1500 cm^{-1} (purine and pyrimidine ring vibration), 1500–1250 cm^{-1} (DNA backbone; base–sugar vibration) and 1250–800 cm^{-1} (deoxyribose stretching, symmetric and asymmetric phosphate groups). The FTIR spectra of NO-DNA showed peaks at 894, 1217, 1490, and 1714 cm^{-1}, which are quite close to that of nCT-DNA. Whereas, the FTIR spectra of 4-Cl-OPD-DNA showed a slight change in the deoxyribose ring vibration (896 cm^{-1} to 899 cm^{-1}), a shift of 3 cm^{-1} was observed when DNA was treated with 4-Cl-OPD. The signal at 1217 cm^{-1} was shifted to 1220 (a shift of 3 cm^{-1}), indicating changes in the phosphate asymmetric stretching of the DNA backbone. No significant shift was observed in the region corresponding to cytosine ring vibrations, 1493 cm^{-1} to 1492 cm^{-1}. The absorption signal at 1713 cm^{-1} shifted to 1709 cm^{-1} in the 4-Cl-OPD-DNA, signifying slight vibrational shifts of guanine residues (Table 1). More pronounced changes were seen in the case of 4-Cl-OPD-NO-DNA, where the signal for deoxyribose shifted from 896 to 901 cm^{-1} (5 cm^{-1} shift). 1217 to 1223 cm^{-1} (6 cm^{-1} shift) and 1713 to 1707 cm^{-1} (6 cm^{-1} shift); no significant shift in wavelength of the signature peak for cytosine residues was found (Fig. 3).

Free radical quenching assays

Free radical quenchers were used to identify the type of free radicals involved in modifying the DNA treated with DEANO or 4-Cl-OPD and in combination. 47 and 35% inhibition was observed when SOD was used as a scavenger in case of 4-Cl-OPD and 4-Cl-OPD with DEANO treatment respectively. When PTIO (nitric oxide trapping agent) was used as the quencher, strong inhibition was achieved in 4-Cl-OPD-NO-DNA samples (51%) and only 6% in the case of DNA treated with 4-Cl-OPD alone. No significant inhibition in modifications was seen in 4-Cl-OPD-DNA and 4-Cl-OPD-NO-DNA when scavengers for hydroxyl radicals were used (DMSO and D-mannitol), suggesting, hydroxyl radicals are not involved in either of the conditions. Antioxidants like uric acid and ascorbic acid were also used as quenchers and showed significant inhibition in the modifications. The modifications in 4-Cl-OPD-DNA and 4-Cl-OPD-NO-DNA were inhibited by 31% and 42%, respectively, in presence of uric acid, whereas the inhibition was around 33% and 39%, respectively, with ascorbic acid. The results indicate superoxide to be the main radical involved in modifications of 4-Cl-OPD-DNA. In the presence

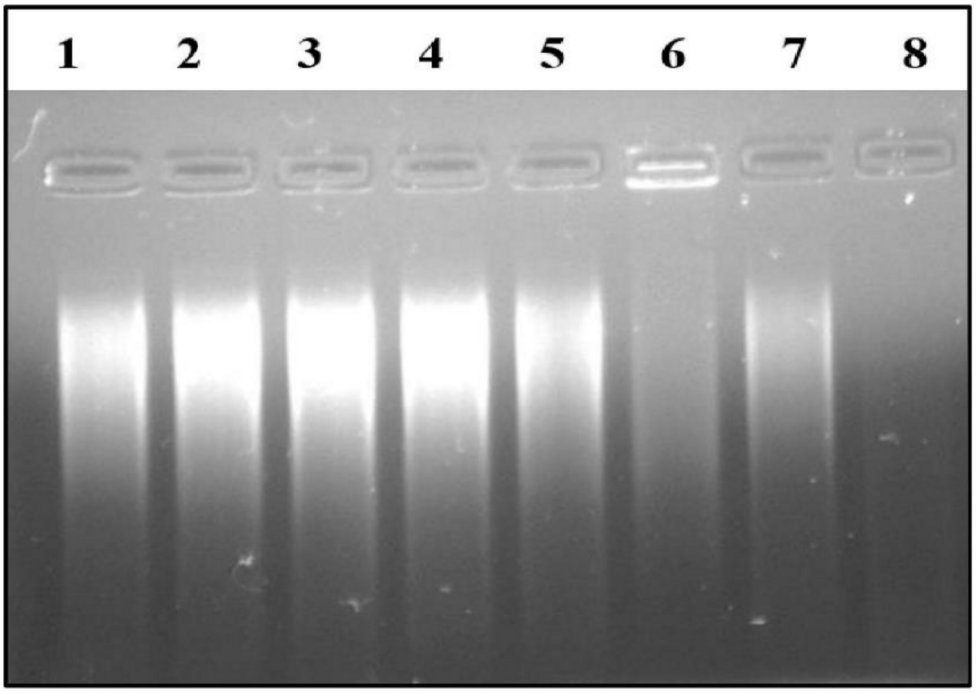

Fig. 2. Nuclease S1 digestion assay. Lane 1: nCT-DNA; lane 2: nCT-DNA + S1 nuclease; lane 3: NO-DNA; lane 4: NO-DNA + S1 nuclease; lane 5: 4-Cl-OPD-DNA; lane 6: 4-Cl-OPD-DNA + S1 nuclease; lane 7: 4-Cl-OPD-NO-DNA; lane 8: 4-Cl-OPD-NO-DNA + S1 nuclease. S1 digestion was carried out at 20 units/μg DNA. Each lane contains 1 μg of DNA.

FTIR wave numbers in cm^{-1}				
DNA samples	**Deoxyribose ring vibrations**	**Symmetric and asymmetric phosphate group stretching**	**Cytosine ring vibrations**	**Guanine ring vibrations**
nCT-DNA	896	1217	1493	1713
NO-DNA	894	1217	1490	1714
4-Cl-OPD-DNA	899	1220	1492	1709
4-Cl-OPD-NO-DNA	901	1223	1491	1707

Table 1. Shift in FTIR wave numbers for different modified forms of DNA.

of superoxide radicals, nitric oxide may produce peroxynitrite that could act as the main culprit for alterations in the DNA molecule when treated with both 4-Cl-OPD and NO donor (Fig. 4).

High-performance liquid chromatography (HPLC) of native DNA and DNA treated with 4-Cl-OPD, DEANO, and combined action of DEANO and 4-Cl-OPD

The HPLC chromatograms of standard 8-hydroxy-2′-deoxyguanosine and 8-nitroguanine show a retention time of 10.515 and 9.183 (Fig. 5A and B, respectively). HPLC chromatogram of acid-hydrolyzed nCT-DNA gave peaks at a retention time of 4.866, 5.741, and 7.75 min (Fig. 5C). While NO-DNA gave peaks at 4.283, 5.83, and 8.57 min (Fig. 5D), indicating no significant change. The acid hydrolysates of 4-Cl-OPD-DNA showed peaks at 4.083 and 5.233 min, and an additional peak at 10.288 min was seen (Fig. 5E); this new peak corresponds to 8-oxo-dG formation. The hydrolyzed 4-Cl-OPD-NO-DNA sample gave peaks at a retention time of 4.158, 5.291, 9.308, and 10.691 min (Fig. 5F). An additional peak at 9.308 min in the 4-Cl-OPD-NO-DNA sample is characteristic of 8-nitroguanine formation.

Immunological studies on antibodies isolated from the sera of cancer patients

Screening of circulating peripheral cancer antibodies with native and modified forms of DNA through direct binding ELISA

The sera from cancer patients (n = 264) were grouped according to the type of cancer. ELISA was performed on all the groups, i.e. non-Hodgkin's lymphoma; NHL (n = 27), Hodgkin's lymphoma; HL (n = 30), hepatocellular carcinoma; HCC (n = 35), cervical cancer; CVC (n = 30), urinary bladder cancer; UBC (n = 33), lung cancer; LC (n = 29), breast cancer; BRC (n = 29), prostate cancer; PC (n = 25), and gall-bladder cancer; GBC (n = 26) (Fig. 6). Normal human serum served as control. Cancer antibodies from hepatocellular carcinoma and urinary bladder cancer showed high binding with the modified forms of DNA i.e., 4-Cl-OP-DNA and 4-Cl-OPD-NO-

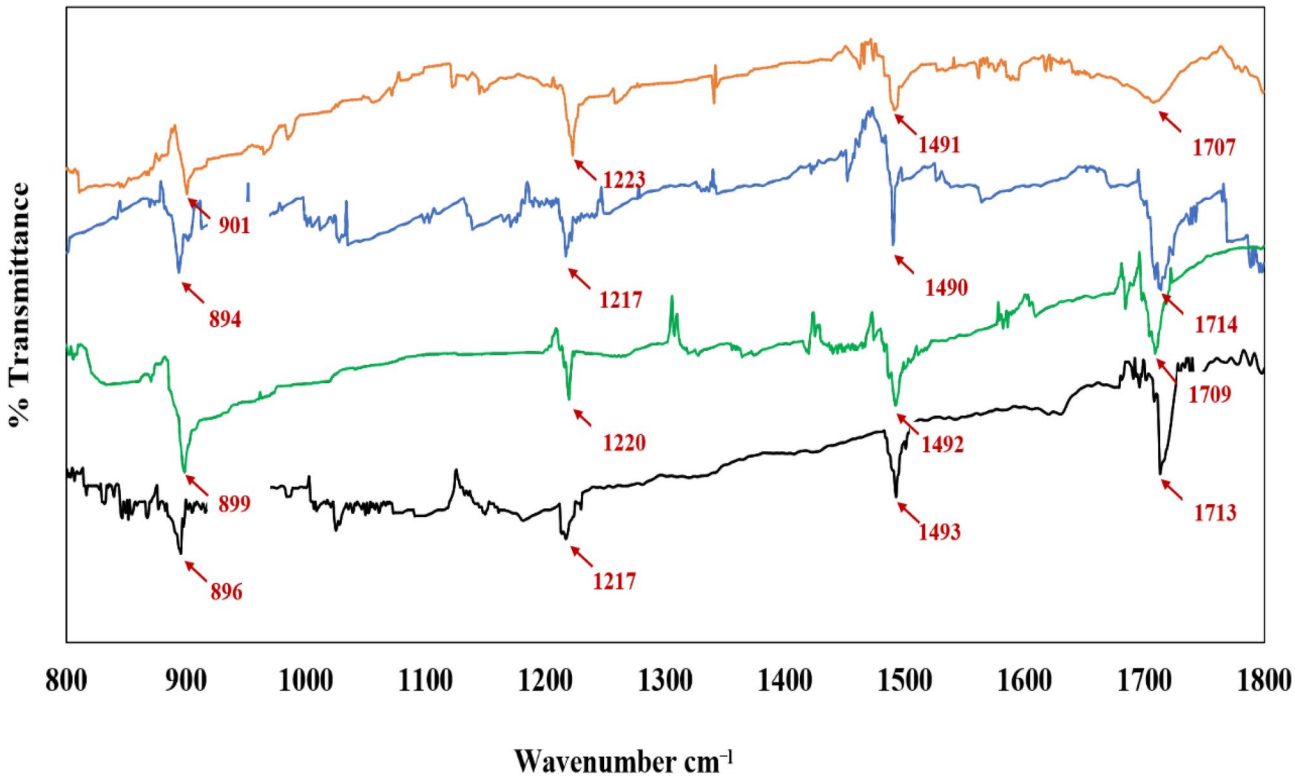

Fig. 3. FTIR spectra of nCT-DNA (-), 4-Cl-OPD-DNA (green hyphen), NO-DNA (blue hyphen), and 4-Cl-OPD-NO-DNA (brown hyphen).

DNA, with a p-value of < 0.0001 in both cases. However, on comparing the level of binding specificity between HCC and UBC, the hepatocellular carcinoma IgG showed significantly higher binding in the order 4-Cl-OPD-NO-DNA (p-value < 0.0001) > 4-Cl-OPD-DNA (p-value $= 0.0006$). ELISAs performed on antibodies present in the sera of non-Hodgkin's lymphoma, Hodgkin's lymphoma, cervical, lung, gall bladder, prostate, and breast cancer did not show appreciable binding with either of the modified forms of DNA (Fig. 6A).

To access and quantify the specificity of cancer autoantibodies towards epitopes induced on the DNA molecule because of treatment with DEANO or 4-Cl-OPD, and DEANO along with 4-Cl-OPD, competition ELISA was performed on the IgG extracted from the sera of the high binding group of cancers i: e, Hepatocellular carcinoma, and urinary bladder cancer. This binding was followed by the lung cancer sera group although it was not significant, but we have included this group along with HCC and UBC group for further analysis.

Isolation of IgG from the sera of the hepatocellular, urinary bladder, and lung carcinoma patients

The antibodies were isolated with the help of the Protein-A agarose affinity column, the normal human sera, and the sera of patients with hepatocellular carcinoma, urinary bladder, and lung cancers were used here. A single peak of purified IgG was observed at 280 nm (Fig. 6B).

The serum samples showing high binding in direct binding ELISA were pooled for IgG isolation.

Estimation of the binding specificity of cancer sera/IgGs through competition ELISA

Cancer sera and purified IgG from the sera of hepatocellular carcinoma, urinary bladder, and lung cancer patients were assessed for their binding specificity towards nCT-DNA and the modified DNAs by competitive inhibition ELISA.

When 4-Cl-OPD-DNA was used as an inhibitor in increasing concentrations (0 to 20 µg/ml), the maximum inhibition obtained was $42.5 \pm 2.39\%$, $36.01 \pm 4.1\%$ and 34.82 ± 2.8 at 20 µg/ml of the inhibitor for hepatocellular carcinoma, urinary bladder, and lung cancer sera respectively. However, when 4-Cl-OPD-NO-DNA was used as an inhibitor at 20 µg/ml, an inhibition of $57.5 \pm 2.46\%$, $44.6 \pm 4.03\%$, and 33.98 ± 3.32 was obtained for hepatocellular carcinoma, urinary bladder, and lung cancer sera respectively (Table 2).

Competition ELISA performed using IgG from hepatocellular carcinoma, urinary bladder, and lung cancer patients' sera showed inhibition of $44.78 \pm 2.52\%$, $39.66 \pm 1.21\%$, and $33.51 \pm 2.0\%$, respectively, at 20 µg/ml 4-Cl-OPD as an inhibitor. However, in the case when 4-Cl-OPD-NO-DNA was used as an inhibitor, an inhibition of $56.46 \pm 2.25\%$, $46.57 \pm 1.54\%$, and 35.44 ± 1.22 was achieved with the respective IgGs (Table 3).

Estimation of total serum nitrite levels in patients with hepatocellular, urinary bladder, and lung cancer

For estimation of serum nitrite, the cancer patients were divided into three age groups: Group I (20–30 years), Group II (31–40 years), and Group III (41–50 years). The total serum nitrite level in Group I was

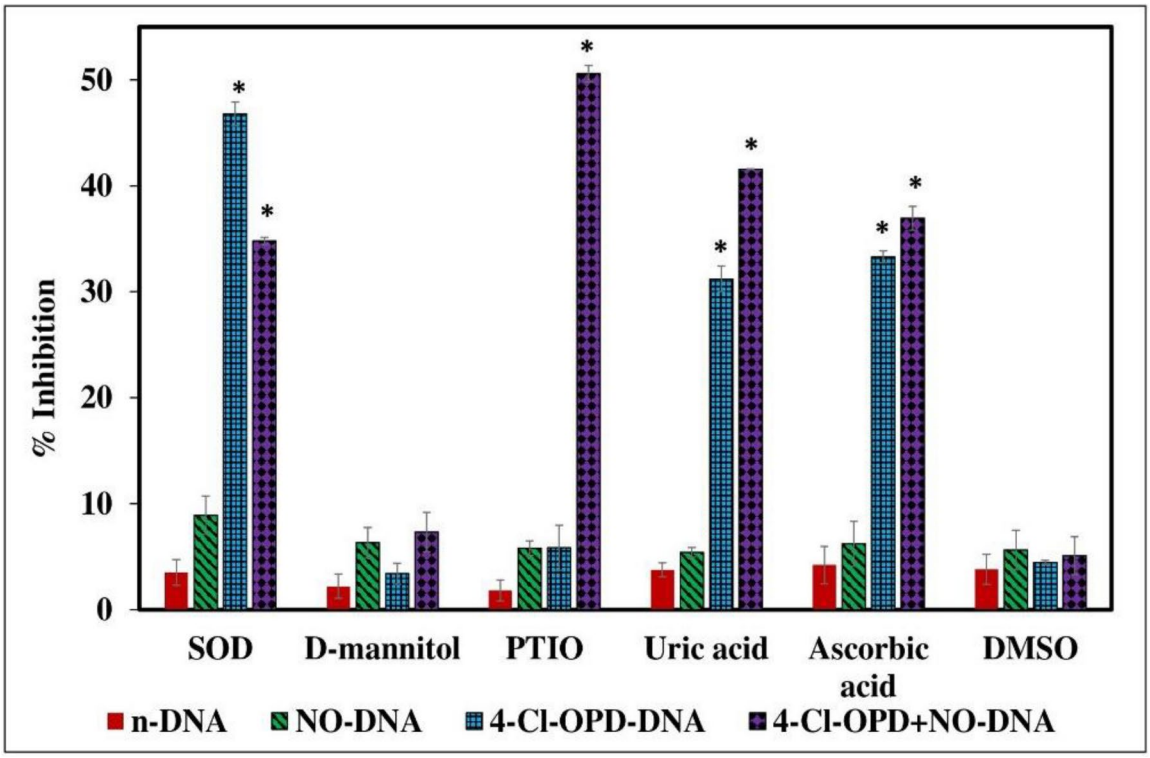

Fig. 4. Effect of free radical scavengers, antioxidants, and NO-trapping agent on the modification of DNA induced by 4-Cl-OPD and DEANO (NO donor molecule). The NO-trapping agent (PTIO), superoxide radical scavenger (SOD), hydroxyl radical scavenger (DMSO and D-mannitol), and antioxidants (ascorbic acid and uric acid) were used at different concentrations. Each bar represents the mean ± SD of 3 independent assays. *p-value of < 0.05 was considered statistically significant.

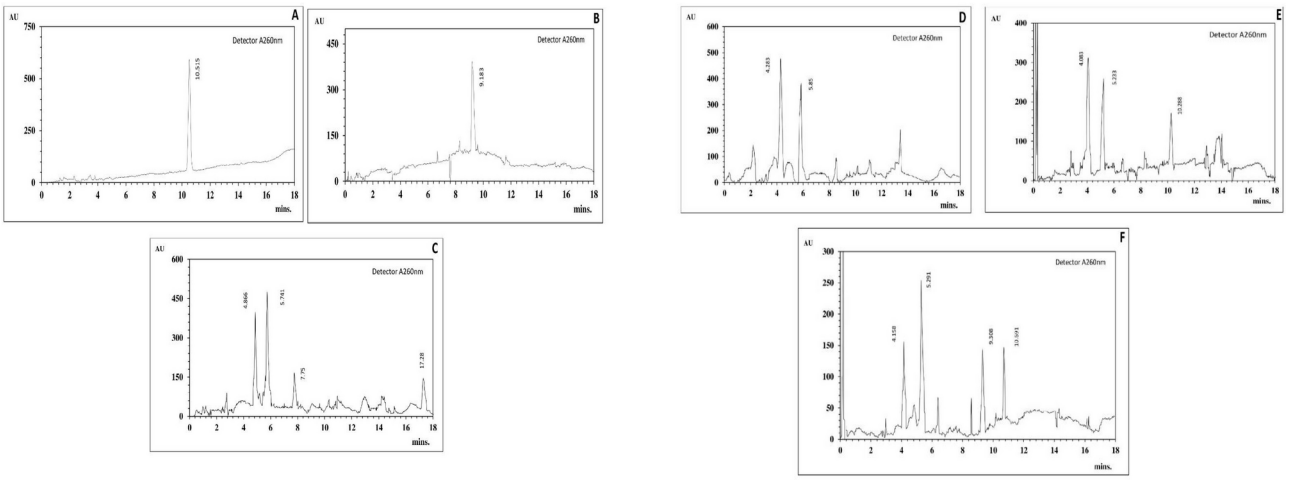

Fig. 5. HPLC chromatogram of standard 8-hydroxy-2′deoxyguanosine (**A**), standard 8-nitroguanine (**B**), acid hydrolyzed nCT-DNA (**C**), acid hydrolyzed NO-DNA (**D**), acid hydrolyzed 4-Cl-OPD-DNA (**E**) and acid hydrolyzed 4-Cl-OPD-NO-DNA (**F**).

48.33 ± 2.08 µmol/l, 45.66 ± 0.56 µmol/l, and 42.56 ± 1.95 for hepatocellular carcinoma, urinary bladder, and lung cancer, respectively. The serum nitrite for the control was found to be 24.6 ± 0.471 µmol/l. In group II, the nitrite levels were 51.67 ± 3.72 µmol/l, 52.33 ± 0.57 µmol/l, and 52.45 ± 3.53 µmol/l, respectively. The nitrite level in the sera of this control group was 22.5 ± 1.52 µmol/l. In Group III, the nitrite levels were 55.66 ± 1.15 µmol/l, 52.8 ± 1.154 µmol/l, and 51.34 ± 2.27 µmol/l, respectively. In the control samples, it was found to be 21.32 ± 1.73 µmol/l (Fig. 7).

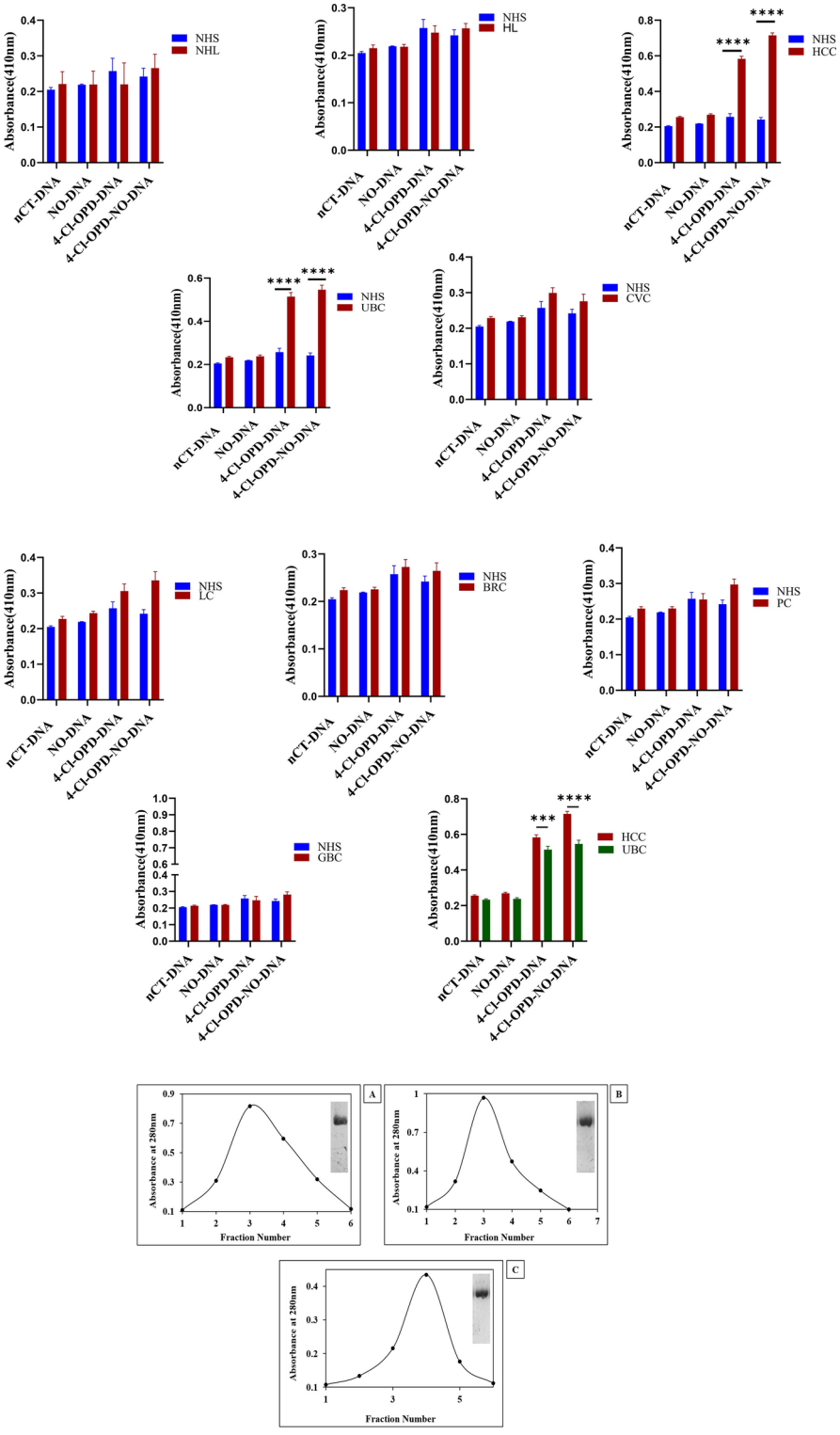

Fig. 6. (**A**) Direct binding ELISA of normal human sera (NHS) and various cancer patients' sera i.e., non-Hodgkin's lymphoma (NHL), Hodgkin's lymphoma (HL), hepatocellular carcinoma (HCC), cervical cancer (CVC), urinary bladder cancer (UBC), lung cancer (LC), breast cancer (BRC), prostate cancer (PC), and gall-bladder cancer (GBC) to nCT-DNA, NO-DNA, 4-Cl-OPD-DNA, and 4-Cl-OPD-NO-DNA and comparative statistical analysis between HCC (brown colour filled square) and UBC (green colour filled square) antisera for higher binding specificity. The ELISA immuno-modules were coated with the respective antigens (2.5 µg/ml). Statistical significance was calculated using two-way ANOVA- Sidak's multiple comparison test, and results were presented as mean ± SEM, $^{****}p < 0.0001$; $^{***}p = 0.0006$. (**B**) Elution profile of IgG obtained from Hepatocellular carcinoma (**A**), Urinary bladder cancer (**B**), and lung cancer (**C**) patients' sera on a protein-A agarose affinity column. Inset represents the purification band for the IgG molecule on SDS-PAGE.

The type of serum sample used	The number of sera analyzed in each group[#]	Inhibitor used and mean percent inhibition calculated at 20 µg/ml of inhibitor ± standard deviation			
		nCT-DNA	NO-DNA	4-Cl-OPD-DNA	4-Cl-OPD-NO-DNA
Normal human sera (NHS)	50	24.45 ± 2.55	22.54 ± 4.05	25.84 ± 3.5	28.69 ± 2.68
Hepatocellular carcinoma	32	32.6 ± 1.9	31.5 ± 3.2	42.5 ± 2.39	57.5 ± 2.46
Urinary bladder cancer	26	30.65 ± 3.8	29.5 ± 2.8	36.01 ± 4.1	44.6 ± 4.03
Lung cancer	14	26.38 ± 3.6	27.89 ± 4.21	34.82 ± 2.8	33.98 ± 3.32

Table 2. Competition ELISA of circulating antibodies in normal human sera and sera from hepatocellular carcinoma, urinary bladder cancer, and lung cancer patients with nCT-DNA, NO-DNA, 4-Cl-OPD-DNA, and 4-Cl-OPD-NO-DNA at 20 µg/ml of the respective antigen. [#]The number of sera includes high responders in direct binding ELISA.

IgG samples	Number of pooled IgGs[#]	Inhibitor used and percent inhibition calculated at 20 µg/ml of inhibitor ± standard deviation			
		nCT-DNA	NO-DNA	4-Cl-OPD-DNA	4-Cl-OPD-NO-DNA
Normal human IgG	25	25.6 ± 0.967	24.39 ± 1.58	25.8 ± 1.95	26.89 ± 1.5
Hepatocellular carcinoma IgG	22	27.68 ± 1.22	27.73 ± 1.06	44.78 ± 2.52	56.46 ± 2.25
Urinary bladder cancer IgG	13	26.9 ± 1.92	25.53 ± 1.63	39.66 ± 1.21	46.57 ± 1.54
Lung cancer IgG	12	25.78 ± 1.8	26.74 ± 2.34	33.51 ± 2.0	35.44 ± 1.22

Table 3. Competition ELISA of IgG isolated from normal human sera, hepatocellular carcinoma, urinary bladder, and lung cancer sera with nCT-DNA, NO-DNA, 4-Cl-OPD-DNA and 4-Cl-OPD-NO-DNA at 20 µg/ml of the respective antigen. [#]IgGs from sera showing appreciable interaction in direct binding ELISA were pooled.

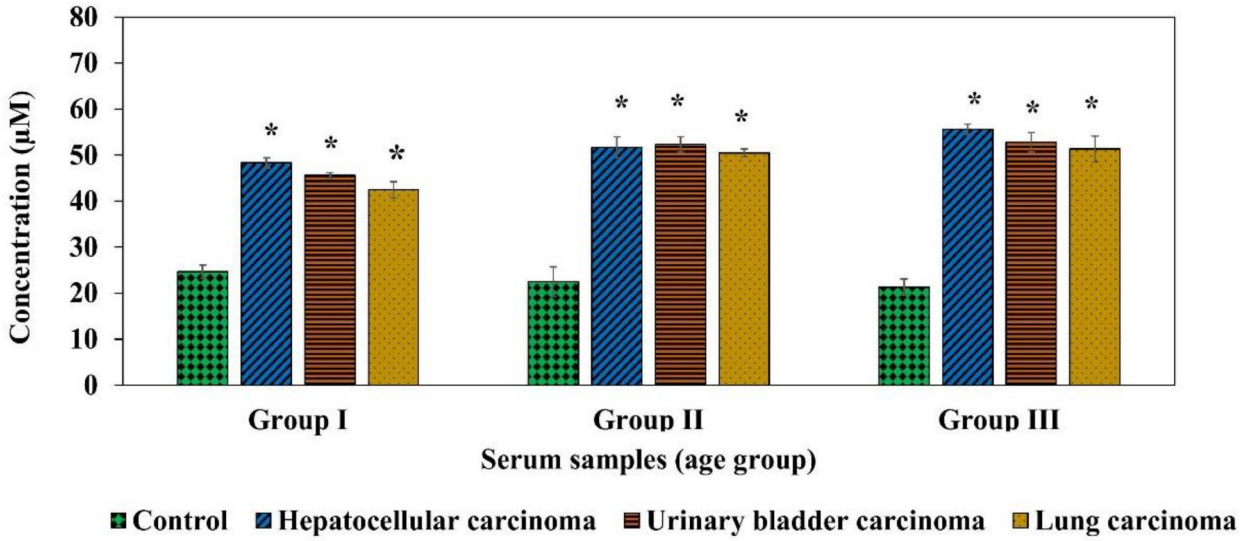

Fig. 7. Serum nitrite levels in normal human serum (NHS), hepatocellular carcinoma, urinary bladder carcinoma, and lung carcinoma patients' sera. Each bar represents the mean ± SD of 3 independent assays. *p-value of < 0.05 was considered statistically significant.

Detection of the antigen–antibody complex by electrophoretic mobility shift assay (EMSA)

IgG isolated from hepatocellular carcinoma patients showed the highest binding with modified forms of DNA in direct binding and competition ELISA. The serum nitrite level was also the highest for this case. So, to visualize the antigen–antibody complex formation between the pooled hepatocellular carcinoma IgG and the modified DNA samples, EMSA was performed.

To prepare the antigen–antibody complex, a constant amount of nCT-DNA or the modified DNA (0.5 µg) was incubated with increasing concentrations of IgG (0–60 µg). The samples were then electrophoresed, and the formation of the immune complex was observed in the gel by retarded mobility of the DNA band, mainly due to high molecular weight complexes formation. The retardation in the mobility was seen in the form of

bright fluorescent bands in the case of the 4-Cl-OPD-DNA-IgG complex (Fig. 8B) and 4-Cl-OPD-NO-DNA-IgG complex (Fig. 8D). However, no immune complex formation was observed when hepatocellular carcinoma IgG was allowed to interact with nCT-DNA or NO-DNA (Fig. 8A and C). EMSA for urinary bladder cancer antibodies also showed the formation of immune complexes with 4-Cl-OPD-DNA and 4-Cl-OPD-NO-DNA. However, the retardation in the mobility and fluorescence intensity were less compared to hepatocellular carcinoma IgG.

Discussion

Epidemiological studies have provided weak evidence of the link between hair dye use and carcinogenicity[3,5,41–43]. 4-Cl-OPD is a commonly used hair dye precursor in permanent formulations; it is linked to increased ROS production in vitro and in vivo, protein aggregation, genotoxicity, and cytotoxicity[1,21–23]. Studies have documented the increasing use of oxidative synthetic permanent hair-dying formulations in both sexes in the developing and developed world. Imbalanced ROS and enhanced NO production are associated with inflammatory conditions and cancer induction[44–46]. NO is the product of the enzyme nitric oxide synthase (NOS) activity on L-arginine. Among the family of NOS, two are constitutive (neuronal NOS and endothelial NOS), and one is an inducible form (i NOS). i NOS activity increases under stress and allergic responses. Pathologic increase in NO production is associated with many chronic human diseases. NO in the vicinity of ROS results in the generation of reactive nitrogen species (RNS) such as nitrogen dioxide (NO_2), peroxynitrite ($ONOO^-$), and dinitrogen trioxide (N_2O_3)[47–49]. Above the physiological levels, RNS leads to oxidative and nitrosative stress in the system. Peroxynitrite is a potential oxidant that can attack biological macromolecules like proteins, DNA, and lipids, resulting in cellular damage and toxicity[50–52]. DNA damage by ROS and RNS has been widely seen as one of the causes of cancer induction. 8-Oxo-dG and 8-nitroguanine are the markers of oxidative and nitrosative stress to DNA and were detected in various cancerous tissues and have been reported to show implications in cancer biology[53,54].

Studies have documented and supported the role of nitro-oxidative stress-induced modifications and DNA adduct formation as potential biomarkers for studying cancer progression and its prognosis[55,56]. However, the role of 4-Cl-OPD-modified DNA under nitrosative stress in cancer immunology remains unexplored. Therefore, in continuation of our previous work on the effect of 4-Cl-OPD on calf thymus DNA and its characterization, this study aims to understand the synergistic action of 4-Cl-OPD and DEANO on the structure of DNA, detailed characterization of the modified forms of DNA and to probe for the presence of antibodies in a different group

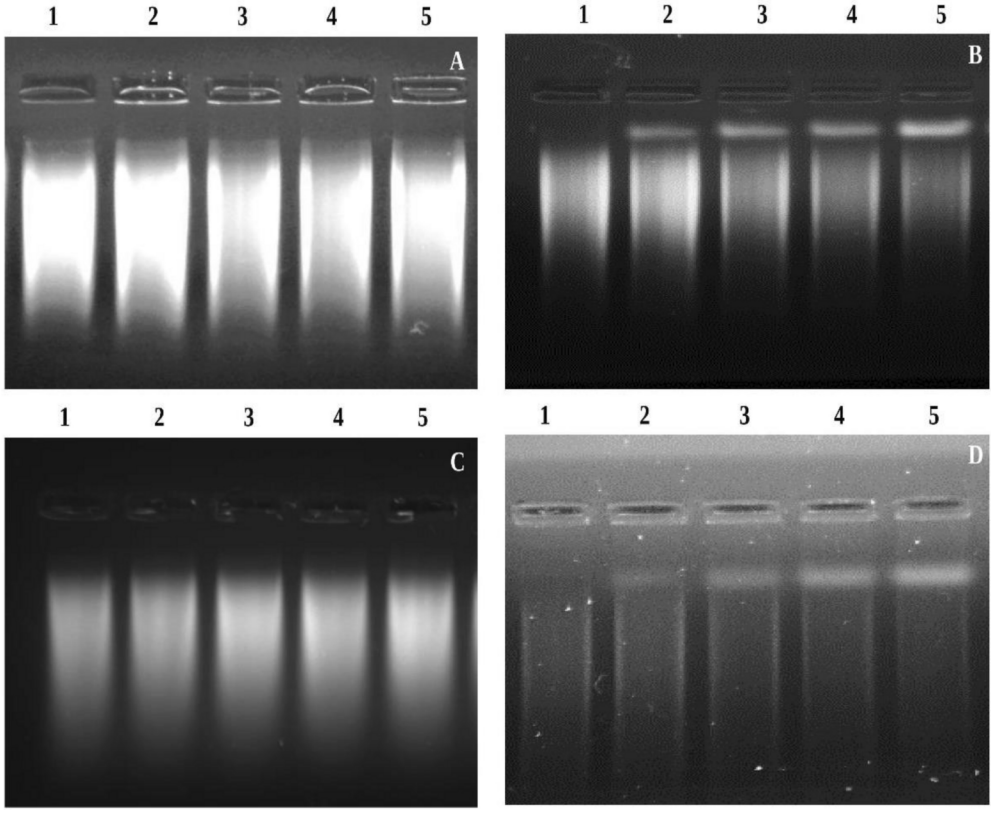

Fig. 8. Electrophoretic mobility shift assay (EMSA) of affinity purified Hepatocellular IgG with (**A**) native calf thymus DNA, (**B**) 4-Cl-OPD-DNA, (**C**) NO-DNA and (**D**) 4-Cl-OPD-NO-DNA, 0.5 µg each was incubated with 0, 10, 20, 40 and 60 µg of isolated hepatocellular carcinoma IgG (lanes 1–5) under similar experimental conditions.

of cancers that could identify the neoepitopes on DNA incited on treatment with 4-Cl-OPD and DEANO (NO donor). UV–vis spectroscopy of the modified forms of DNA showed significant hyperchromicity at 260 nm with a slight shift in wavelength pointing towards the exposure of nitrogenous bases due to the disruption of hydrogen bonding between the base pairs[57]. A second small peak at 400 nm was observed in the case of 4-Cl-OPD-NO-DNA that may correspond to the formation of 8-nitroguanine[52,58–60]. These findings are in agreement with Pacher et al., where they have reported, NO as a fundamental mediator of cellular and macromolecular damage under different conditions. The same study reported that most of the cytotoxicity attributed to NO is due to peroxynitrite, produced from the reaction between NO and some other free radicals. They have also reported the role of NO and peroxynitrite in chronic inflammatory diseases and cancer. The formation of single-stranded regions in DNA could be another reason for increased absorption in the UV–vis region. Single-stranded regions in the DNA molecule do not allow the fluorescent probe, ethidium bromide intercalation. As a result, less fluorescent intensity of the modified DNA could be seen[61]. Quenching of fluorescence in the case of 4-Cl-OPD-DNA and 4-Cl-OPD-NO-DNA could be due to the unwinding of the helical structure of DNA as a result of the disruption of hydrogen bonding and base modifications[62]. NO alone does not appear to be responsible for any structural alterations in the DNA molecule. However, in the presence of 4-Cl-OPD, NO synergistically led to alterations in the DNA. These changes were quite pronounced as compared to the changes induced by 4-Cl-OPD alone. Indicating that the modifications appear governed by the local concentration of NO.

The generation of single-strand breaks in modified DNA was confirmed by the increased migration and decreased fluorescence of the bands in the S1 nuclease digestibility assay. S1 nuclease cleaves single-stranded DNA regions but not dsDNA; the digested fragments migrate faster in the gel than dsDNA[63]. The increased migration of the modified DNA upon treatment with S1 nuclease indicates the presence of single-stranded regions in the modified forms of DNA (4-Cl-OPD-DNA and 4-Cl-OPD-NO-DNA). However, no single-stranded regions were detected in nCT-DNA and NO-DNA. S1 digestion was more pronounced in 4-Cl-OPD-NO-DNA than 4-Cl-OPD-DNA, suggesting that single-strand generation was more under the synergistic action of 4-Cl-OPD and NO due to nitro-oxidative stress[27,64]. The above findings are in corroboration with Murata et al., who have confirmed the DNA damaging and mutagenic action of hair dye components and have reported an association between occupational exposure to hair dyes and the incidence of cancers.

Nitroxidative stress on the DNA is reported to cause the deamination of guanine and cytosine residues. In the case of proteins, nitration of tyrosine residues and the formation of nitro-tyrosine residues have been reported[65]. Free radical scavengers were used to identify the moiety involved in altering the DNA structure when treated with 4-Cl-OPD and DEANO. Superoxide radical was found to be the mediator of DNA damage when 4-Cl-OPD alone was used. Modifications were prevented when SOD was used as an inhibitor in this reaction mixture. However, comparatively lower inhibition was achieved when SOD was used as an inhibitor under the co-incubated conditions (4-Cl-OPD + DEANO). This signifies that the contribution from superoxide radicals in DNA modifications is mediated under both conditions. NO released by DEANO reacts with $O_2^{\cdot-}$ from 4-Cl-OPD to form peroxynitrite ($ONOO^-$). When PTIO was used as an inhibitor of NO under co-incubated conditions, maximum inhibition was achieved. This signifies that $ONOO^-$ appears to be responsible for the DNA modifications under the co-incubated condition. The role of hydroxyl radicals in DNA modification was not observed.

The structural alterations observed in DNA at the molecular level were further supported by FTIR spectroscopy. Here, the focus is on the vibrations for purine and pyrimidine rings, symmetric and asymmetric phosphate groups, and DNA base-sugar vibrations[66]. The shift in wave number 1713 cm^{-1} of nCT-DNA to 1709 cm^{-1} in the case of 4-Cl-OPD-DNA was observed, and a peak shift at 1707 cm^{-1} in the case of 4-Cl-OPD-NO-DNA indicates a disrupted stacking of the guanine residues, specifically at the minor groove. The phosphate asymmetric vibrations of the DNA backbone and deoxyribose ring vibrations of sugar moiety are represented by 1217 cm^{-1} and 896 cm^{-1}, respectively, for the nCT-DNA. A shift towards a higher wavenumber was observed in the case of 4-Cl-OPD (1220 cm^{-1} and 899 cm^{-1}) and 4-Cl-OPD-NO-DNA (1223 cm^{-1} and 901 cm^{-1}). It points toward the changes in guanine double bond plane stretching vibrations. Indicating the interaction of 4-Cl-OPD and NO with the backbone phosphate groups and DNA's sugar moiety. These shifts in the peak also represent perturbations in the secondary structure of the DNA, from syn to anti, and appear closer to the B′-heteronomous conformation. Cytosine residues were found to be intact and unaltered. This shows that 4-Cl-OPD and NO do not interact with the cytosine of DNA molecules[66,67].

The changes observed in the structure of 4-Cl-OPD, and 4-Cl-OPD-DNA were attributed to oxidative and nitro-oxidative stress on the DNA molecule. This was confirmed by HPLC analysis. The detection of 8-oxo-dG was observed in the case of 4-Cl-OPD-DNA, and both 8-oxo-dG and 8-nitroguanine in the 4-Cl-OPD-NO-DNA sample, the markers of oxidative and nitrosative stress, respectively. Neither peak was detected in the case of NO-DNA and nCT-DNA[68].

Earlier findings have shown the formation of 8-oxo-dG and 8-nitroguanine under oxidative and nitrosative stress in vitro and under various pathological conditions like diabetes mellitus, atherosclerosis, cancer, etc.[58,69,70]. The formation of oxidative and nitro-oxidative DNA lesions may indicate the possible harm synthetic hair dye users face and their vulnerability to developing a chronic inflammatory illness. The above findings are reinforced by the investigations reported by Hiraku & Kawanishi, who stated that 8-nitroguanine is formed at the sites of carcinogenesis regardless of etiology. 8-nitroguanine has the possibility of being used as a potential biomarker to evaluate the risk of inflammatory carcinogenesis.

Another aspect of this study was exploring the possible role of 4-Cl-OPD in cancer progression and determining if DNA modification by oxidative hair dye pigment (4-Cl-OPD) is influenced by nitrosative stress. Strong binding of serum autoantibodies to 4-Cl-OPD-DNA and 4-Cl-OPD-NO-DNA was observed with IgG isolated from the serum of hepatocellular carcinoma, urinary bladder cancer patients. However, no significant binding was seen when the serum of Hodgkin's lymphoma, non-Hodgkin's lymphoma, cervical cancer, lung

cancer, gall bladder, prostate, and breast cancer patients were screened. The sera from the unexposed group did not show significant binding in the direct binding ELISA. Data from NHS, HCC, UBC, and LC is shown in the supplementary material file, Fig. 6-S. This binding appears to result from a robust humoral response against the neo-epitopes on 4-Cl-OPD-DNA and 4-Cl-OPD-NO-DNA because of enhanced and prolonged nitro-oxidative stress. If it persists in the human system, it may compromise the body's antioxidant defense system and increase the chances of progressive DNA damage[71]. According to Ma, environmental or metabolic toxicants produce reactive oxygen and nitrogen species that cause oxidative stress and are viewed as harmful. Hair dyeing components should be viewed under the category of potentially harmful chemicals leading to altered defense status of the living system.

The serum nitrite levels in the normal human system were calculated to be within the physiological range (20–25 µM/l). However, the concentration of serum nitrite in the case of hepatocellular carcinoma (48–55 µM), urinary bladder cancer (45–53 µM), and lung cancer (42–51 µM) were observed to be significantly higher than the physiological limits[72]. A study by Ersoy et al. reported serum nitrite levels may be enhanced in patients with chronic inflammatory pathologies. The serum nitrite levels of patients belonging to other groups of cancers were either within the physiological range or somewhat raised. Variations in serum nitrite levels appear to govern the pathological effect of 4-Cl-OPD in long-term synthetic hair dye users. This appears to be one of the causes why some people using synthetic oxidative hair dyes may present with hypersensitivity and immune stimulations leading to carcinogenic induction. Though the application is dermal, the pigment enters circulation[73] and produces superoxide radicals[27,29,33], which may induce nitro-oxidative conditions under prevailing nitrosative stress. The nitro-oxidative environment is reported to modify the macromolecular system of our body, including DNA, and may induce neo-epitopes on the molecule. Consequently, the immune system may be activated to trigger antibody production. Accumulating altered/modified DNA components and DNA-antibody immune complexes may result in cancer progression[8,74].

To confirm the specificity of IgGs from the hepatocellular, urinary bladder, and lung cancer towards neo-epitopes on DNA, competition ELISAs were performed. Notably, the percentage of inhibition achieved with the 4-Cl-OPD-NO-DNA-IgG complex was higher when compared to the 4-Cl-OPD-DNA-IgG in all three cases of cancers. The difference in inhibition in the case of hepatocellular carcinoma between 4-Cl-OPD-NO-DNA and 4-Cl-OPD-DNA when used as an inhibitor was highest (11.68%). The difference of inhibition in the case of urinary bladder and lung cancer was 6.91% and 1.93%, respectively, suggesting the increased chances of developing hepatocellular carcinoma in synthetic hair dye users with elevated serum NO levels. This observed difference in competitive inhibition data signifies that the DNA modified due to nitro-oxidative stress induced by 4-Cl-OPD and NO could trigger an inflammatory humoral response. Accumulation of modified DNA products, antigen–antibody complexes, and activated immune systems could favor carcinogenesis. Recognition of neo-epitopes by cancer antibodies was further confirmed by electrophoretic mobility shift assay through visualization of immune complex formation between modified DNAs and isolated hepatocellular carcinoma IgG. Formation of high molecular weight immune complex with retarded mobility and diminished fluorescence with the increasing concentrations of hepatocellular carcinoma IgG (10–60 µg) and 4-Cl-OPD-NO-DNA (0.5 µg)[75]. However, when nCT-DNA and NO-DNA were used as antigens (here as inhibitors), no such retardation in mobility was observed. The role of oxidative and nitrosative stress in cancer has been reported in earlier studies[76,77]. Findings from the serum analysis are summarized below:

1. *Among the three high-binding groups, serum nitrite levels were highest in the case of hepatocellular carcinoma and lowest for lung cancer patients.*
2. *Cancer antibodies from hepatocellular carcinoma and urinary bladder cancer identified 4-Cl-OPD-NO-DNA more than 4-Cl-OPD-DNA, however, there was no observable difference in the case of lung cancer for these two antigens.*
3. *Antibodies from hepatocellular carcinoma patients identified* 4-Cl-OPD-DNA and 4-Cl-OPD-NO-DNA to the greatest extent, followed by urinary bladder, and lung cancer patients.
4. *Among these three groups,* hepatocellular carcinoma, urinary bladder cancer, and lung cancer patients*, the percentage of cancer patients showing substantial binding was 91.4, 78.7, and 48 respectively* (Table 2).
5. *The percent inhibition observed (Inhibition ELISA) was in the order* hepatocellular carcinoma > urinary bladder cancer > lung cancer.
6. *In the case of lung cancer, compared to* hepatocellular carcinoma, serum nitrite levels, the number of patients showing antibodies against 4-Cl-OPD-DNA and 4-Cl-OPD-NO-DNA, absorbance in direct binding ELISA and binding specificity were lower.

So, we can conclude, that some of the lung cancer patients (14 out of 29) were observed to show the presence of antibodies against 4-Cl-OPD-DNA and 4-Cl-OPD-NO-DNA, but with compromised specificity.

Here, we report chronic hair dye exposure as one of the factors responsible for altering the intricacies of the DNA's molecular structure and inducing neo-epitopes on the molecule. Also, the physiological status of NO may appear to define the susceptibility towards 4-Cl-OPD and, hence, humoral response in persons who prefer synthetic hair dye. The persistent nitro-oxidative stress due to 4-Cl-OPD and NO may induce a heightened immune response against neoepitopes in the nitro-oxidatively modified DNA[58,78–80]. Therefore, chronic hair dye exposure may be identified as a risk to human health. More laboratory investigations are required to establish and strengthen the carcinogenic risk association with oxidative hair dye use.

Materials and methods

Chemicals/reagents

Calf-thymus DNA, 4-Chloro-orthophenylenediamine, diethylamineNONOate sodium salt dihydrate (DEANO), standard 8-hydroxy-2′deoxyguanosine, anti-human- IgG alkaline phosphatase conjugate, ethidium bromide, p-nitrophenyl phosphate, Coomassie Brilliant Blue R250, sodium dodecyl sulfate, Tween-20, agarose, mannitol, 2-Phenyl-4,4,5,5-tetramethylimidazoline-1-oxyl 3-Oxide(PTIO), dimethyl sulfoxide (DMSO) and superoxide dismutase were purchased from Sigma-Aldrich, U.S.A. Protein A-Sepharose CL-4B, nuclease S1, were from GENEI, India. EDTA, uric acid, and ascorbic acid were from Qualigens, India. Polystyrene microtiter flat bottom ELISA plates having 96 wells (7 mm diameter) were purchased from Nunc, Denmark. Acrylamide, ammonium persulphate, bisacrylamide, N, N, N, N-tetramethylethylenediamine (TEMED) were obtained from Bio-Rad Laboratories, U.S.A. Standard 8-nitroguanine was purchased from Cayman Chemicals. All other reagents and chemicals were of the highest analytical grade available.

Modification of calf thymus DNA by 4-Chloro-orthophenylenediamine and DEANO

Native calf thymus DNA (40 µg/ml; 107.4 µM) was incubated with 20 µM DEANO,100 µM 4-Cl-OPD, and 100 µM 4-Cl-OPD and 20 µM DEANO in 1 M PBS, pH 7.4 for 1 h at 37 °C in the presence of EDTA as a metal-ion chelator. After incubation, the reaction mixture was extensively dialyzed against PBS, pH 7.4, to remove the excess DEANO and 4-Cl-OPD. For better understanding, the DNA samples after treatment will be referred to as; NO-DNA, 4-Cl-OPD-DNA, and 4-Cl-OPD-NO-DNA, respectively. The DEANO and 4-Cl-OPD used here are standardized in our laboratory and represent the minimum concentration that induced quantifiable changes in the DNA molecule[22].

Biophysical characterization of the DNA samples

UV–vis and fluorescence spectroscopy

The UV–visible absorption spectra were recorded using a Shimadzu UV-1700 spectrophotometer (Japan) in the wavelength range of 200–400 nm using quartz cuvettes of path length 1 cm, with PBS, pH 7.4, serving as blank.

$$\%hyperchromicity\ at\ 260\ nm = \left(\frac{A_{modified} - A_{native}}{A_{native}}\right) \times 100.$$

Here; $A_{modified}$ = Absorbance at 260 nm of NO-DNA, 4-Cl-OPD-DNA or 4-Cl-OPD-NO-DNA. A_{native} = Absorbance at 260 nm of nCT-DNA.

Fluorescence spectra of the DNA samples were recorded on Shimadzu RF-5301PC (Japan) spectrofluorometer using quartz cuvettes[39,81]. The spectra were recorded from 300 to 700 nm, and the spectral analysis was done based on the following equation using ethidium bromide as an external flour.

$$\%decrease\ in\ fluorescence\ intensity = \left(\frac{FI_{native} - FI_{modified}}{A_{native}}\right) \times 100.$$

FI signifies the fluorescence intensity.

Agarose gel electrophoresis

For preparing the gel, 0.8% agarose was dissolved by heating in TAE buffer, pH 8.0 (40 mM Tris–acetate and 2 mM EDTA). The gel solution was then cooled to around 50 °C, and ethidium bromide (0.5 µg/ml) was added to it for visualization of DNA bands. The gel solution was then poured into gel casting tray, and agarose was allowed to solidify at room temperature[58].

Sample preparation was done by taking 2 µg each of nCT-DNA, NO-DNA, 4-Cl-OPD-DNA, and 4-Cl-OPD-NO-DNA samples with 1/10 volume of sample buffer (0.125% bromophenol blue, 30% Ficoll-400, 5 mM EDTA in TAE, pH 8.0 (electrophoresis buffer). The samples were then loaded in the wells of 0.8% agarose gel and electrophoresed for 2.5 h at 35 mA. The bands were viewed by a UV light-based illuminator and photographed.

S1 nuclease digestibility assay for the assessment of single-stranded regions

Native, NO-DNA, 4-Cl-OPD, and 4-Cl-OPD-NO-DNA samples were checked for the presence of single-stranded regions by nuclease S1 digestion assay[82]. One µg each of nCT-DNA, NO-DNA, 4-Cl-OPD-DNA, and 4-Cl-OPD-NO-DNA samples were mixed with acetate buffer (30 mM sodium acetate, 1 mM zinc sulfate, 100 mM sodium chloride, pH 4.6) and treated with nuclease S1 (20 units/µg DNA). After 30 min at 37 °C, the reaction was stopped by the addition of 1/10 volume of 200 mM EDTA, pH 8.0. The samples were then electrophoresed on 1% agarose gel and stained with ethidium bromide (0.5 µg/ml). The gels were viewed under UV light and photographed[83].

FTIR spectroscopic analysis to identify changes in the characteristic functional groups of the DNA molecule

The FT-IR spectra of nCT-DNA, 4-Cl-OPD-DNA, NO-DNA, and 4-Cl-OPD-NO-DNA were determined on a Perkin-Elmer Spectrum Two FTIR spectrometer (USA). The spectrum was recorded in the wavelength range of 1800–800 cm^{-1} to cover the major absorption bands of DNA[84,85]. Around 10 µl of the native and treated DNA samples were placed on the horizontal attenuated total internal reflection (HATR) crystal, and interferograms were then recorded. The spectra of three independent samples were recorded, and the average result was reported.

Detection of free radicals causing damage to DNA by absorbance quenching studies
Quenching assays were performed to identify the specific type of radicals involved in inducing structural alterations in nCT-DNA upon treatment with DEANO and 4-Cl-OPD and by the combined action of DEANO and 4-Cl-OPD. The quenchers used were superoxide dismutase (SOD, 550 units/ml), hydroxyl radical scavengers (DMSO and D-mannitol at 20 mM each), nitric oxide-trapping agent (carboxy-PTIO at 20 mM) and antioxidants (ascorbic acid at 20 mM and uric acid at 0.05 mM). The effect of the quenchers was studied by incubating the treated DNA (40 µg each) in 0.1 M phosphate-buffered saline, pH 7.4, with 0.1 mM EDTA at 37 °C for 1 h. Absorbance at 260 nm (A_{260}) was recorded for each sample, and percent quenching was calculated[58].

High-performance liquid chromatography of the native DNA and DNA treated with DEANO, 4-Cl-OPD, and combined action of DEANO and 4-Cl-OPD
The HPLC chromatograms of nCT-DNA, NO-DNA, 4-Cl-OPD-DNA, and 4-Cl-OPD-NO-DNA were analyzed on analytical HPLC of Shimadzu Corporation, Japan (Model no. LC-2030 Plus) equipped with a UV–vis multiwavelength detector. The samples were treated with 0.1 N HCl at 110 °C for 24 h to liberate purine residues[86]. The hydrolyzed samples were filtered through a 0.25 µM Milex filter before HPLC analysis. An aliquot of each reaction mixture (20 µl) was run separately on isocratic mode, using a C-18 column and 10% methanol as the mobile phase at a flow rate of 0.5 ml/min[87,88]. NO-DNA, 4-Cl-OPD-DNA, and 4-Cl-OPD-NO-DNA will now be referred to as modified forms of DNA.

Immunological studies on immunoglobulin G isolated from the sera of cancer patients

Collection of sera from cancer patients
Blood was collected from different groups of cancer patients (n = 264), both males and females, of 20 to 50 years of age attending the indoor and outdoor clinic of Jawaharlal Nehru Medical College Hospital (JNMCH), Aligarh, India. The sera were isolated from histologically confirmed malignancies, including non-Hodgkin's lymphoma, NHL (n = 27), Hodgkin's lymphoma, HL (n = 30), hepatocellular carcinoma, HCC (n = 35), cervical cancer, CVC (n = 30), urinary bladder cancer, UBC (n = 33), lung cancer, LC (n = 29), breast cancer, BRC (n = 29), prostate cancer, PC (n = 25), and gall-bladder cancer, GBC (n = 26). Patients receiving any chemo- or radiation therapy, females on hormone replacement therapy, smokers, and patients with co-morbidities were excluded from the study. The patients' selection criteria were based on the history of personal or occupational exposure to dyeing permanent formulations for ≥ 5 years, at least a month. 50 healthy individuals (25 males and 25 females) in the same age group and with a similar history of hair dye use (≥ 5 years, at least a month) served as the control. Sera was also collected from healthy individuals (n = 21) and cancer patients with no hair dye exposure. This study presents data from HCC, UBC, and LC (n = 34) with no history of hair dye exposure. All the study participants were made to sign an informed consent form. The work was duly approved by the Institutional Ethical Committee (IEC), Jawaharlal Nehru Medical College and Hospital, Faculty of Medicine, Aligarh Muslim University, India. Under National Ethics Committee Registry for Biomedical and Health Research, NECRBHR DHR ICMR and Central Drugs Standard Control Organization (CDSCO) Ministry of Health and Family Welfare, Govt. of India. (IEC, D.No. 1043/FM, dated: 11.08.2018). The IEC committee has reviewed and approved all the experiments that were carried out on human blood samples. The study has followed all the relevant guidelines/regulations involving human subjects and was performed in accordance with the Declaration of Helsinki. The serum samples were de-complemented by heating at 56 °C for 30 min and stored at − 20 °C with 0.2% sodium azide[79].

Estimation of total serum nitrite in cancer and normal human system
The NO level in a biological sample is equal to its total nitrite. This total nitrite can be estimated by reaction with Griess reagent [1% sulphanilamide, 0.1% N-(1-naphthyl) ethylenediamine dihydrochloride][89]. The serum samples were first treated with vanadium (III) chloride to convert all the nitrate into nitrite, and then Griess reagent was added. A purple adduct is formed whose absorbance was read at 548 nm. $NaNO_2$ (0–100 µmol/l) was used to construct a standard plot[90,91].

Direct binding enzyme-linked immunosorbent assay (ELISA)
Sera isolated from normal healthy subjects (NHS) serving as a control and cancer patients were tested for antibodies that could identify epitopes on nCT-DNA, NO-DNA, 4-Cl-OPD-DNA, and 4-Cl-OPD-NO-DNA Direct binding ELISA was carried out on polystyrene-coated flat bottom maxisorp microtiter modules. The modules were coated with 100 µl of native and modified DNA samples at a concentration of 2.5 µg/ml and kept for two hours at 37 °C followed by overnight incubation at 4 °C. Extensive washing was done by TBS-T (20 mM Tris, 2.68 mM KCl, and 150 mM NaCl, containing 0.05% of Tween-20) pH 7.4. Nonspecific and unoccupied sites in the wells were blocked with 200 µl of 1.5% bovine serum albumin (BSA) dissolved in TBS (10 mM Tris, 150 mM NaCl) pH 7.4 and kept at 37 °C for 6 h, then overnight at 4 °C. Bound antibodies were analyzed using anti-human-IgG alkaline phosphatase conjugate and p-nitrophenyl phosphate (PNPP) as a substrate. The ELISA modules were then read at 410 nm on an ELISA microplate reader, Bio-Rad, Japan (Model No. iMark, 10630). The results are reported as the mean of the duplicate wells using appropriate controls[79,92].

Isolation and characterization of IgG using protein A- agarose affinity column
IgG was isolated using protein A agarose column[93,94]. The isolated IgG was characterized for antigen (DNA) interaction through competition ELISA and electrophoretic mobility assay. IgG concentration was determined by considering the absorbance of 1.4 at 278 nm equivalent to 1.0 mg IgG/ml. The isolated IgG was dialyzed against PBS and stored at − 20 °C with 0.1% sodium azide for further analysis.

Competitive inhibition ELISA

After screening through direct binding ELISA, the specificity of antigen–antibody interaction (here, DNA-IgG) was quantified through competition ELISA. Varying concentrations of inhibitors (0–20 µg/ml) and a constant amount of IgG (50 µg/ml) were allowed to interact for 2 h at 37 °C, then overnight at 4 °C. The immune complex formed was added to respective antigen-adsorbed modules. The rest of the procedure was the same as described for the direct binding ELISA. The results represent an average of the duplicate wells with ± standard deviation[79]. Percent inhibition was calculated using the formula:

$$\%inhibition = \left(1 - \frac{A_{inhibited}}{A_{uninhibited}}\right) \times 100.$$

Electrophoretic mobility shift assay (EMSA) for visualization of antigen–antibody interaction

The formation of an immune complex via antigen–antibody binding was visualized by the electrophoretic mobility shift assay[95,96]. Constant amounts of native and modified CT-DNAs were incubated with varying amounts of affinity-purified IgG in TBS at 37 °C for 2 h and then overnight at 4 °C. Sample dye was added, and electrophoresis was performed on 1% agarose gel for 3 h at 35 mA. Gel preparation and visualization were done as described previously in the agarose gel electrophoresis section.

Statistical analysis

All experiments were done in triplicates. Student's *t*-test or 2way ANOVA-Sidak's multiple comparison test with 95.00% CI of difference was applied to evaluate differences using the GraphPad InStat software program (GraphPad Software, Inc.).

Conclusions

The synthetic hair dye component 4-Cl-OPD can oxidatively modify DNA and, in the presence of NO, can lead to nitro-oxidatively modified DNA products; these components act as neo-antigens for the immune system to trigger antibody production. Elevated serum levels of nitric oxide, accumulating nitro-oxidatively modified DNA products, and persistent immune complex formation may increase the susceptibility of hepatocellular carcinoma in persons exposed to hair dyeing formulations rich in 4-Chloro-ortho phenylenediamine, either personally or professionally. Regarding previous research and the findings of this work, a compelling argument can be made for further investigations to elucidate the impact of hair dye components on human biology and to understand the role of altered NO status in chronic diseases like cancer.

Data availability

The agarose gel, PAGE in original uncropped form, direct binding ELISA of the non-exposed group has been submitted as a supplementary file. Other raw data supporting this study's findings will be made available from the corresponding author upon reasonable request.

Received: 8 December 2023; Accepted: 7 October 2024
Published online: 11 November 2024

References

1. Weisburger, K., Murthy, S., Fleischman, W. & Hagopian, M. Carcinogenicity of 4-Chloro-o-phenylenediamine, 4-Chloro-m-phenylenediamine, and 2-Chloro-p-phenylenediamine in Fischer 344 rats and B6C3F1 mice. *Carcinogenesis* **6**, 495–499. https://doi.org/10.1093/carcin/1.6.495 (1980).
2. White, J. et al. Adolescent use of hair dyes, straighteners and perms in relation to breast cancer risk. *Int. J. Cancer* **9**, 2255–2263. https://doi.org/10.1002/ijc.33413 (2021).
3. Zhang, Y. et al. Personal use of permanent hair dyes and cancer risk and mortality in US women: prospective cohort study. *BMJ* **370**, m2942. https://doi.org/10.1136/bmj.m2942 (2020).
4. Cho, A., Oh, E., Lee, E. & Sul, D. Effects of hair dyeing on DNA damage in human lymphocytes. *J. Occup. Health* **6**, 376–381. https://doi.org/10.1539/joh.45.376 (2003).
5. Towle, M., Grespin, E. & Monnot, D. Personal use of hair dyes and risk of leukemia: a systematic literature review and meta-analysis. *Cancer Med.* **10**, 2471–2486. https://doi.org/10.1002/cam4.1162 (2017).
6. Ali, A. et al. Risk of carcinogenicity associated with synthetic hair dyeing formulations: A biochemical view on action mechanisms, genetic variation and prevention. *Indian J. Clin. Biochem.* **4**, 399–409. https://doi.org/10.1007/s12291-022-01051-x (2022).
7. Tafurt-Cardona, Y., Suares-Rocha, P., Fernandes, C. & Marin-Morales, A. Cytotoxic and genotoxic effects of two hair dyes used in the formulation of black color. *Food Chem. Toxicol.* **86**, 9–15. https://doi.org/10.1016/j.fct.2015.09.010 (2015).
8. IARC Working Group on the Evaluation of Carcinogenic Risks to Humans. Some nitrobenzenes and other industrial chemicals (International Agency for Research on Cancer 2020).
9. Seydi, E., Fatahi, M., Naserzadeh, P. & Pourahmad, J. The effects of para-phenylenediamine (PPD) on the skin fibroblast cells. *Xenobiotica* **10**, 1143–1148. https://doi.org/10.1080/00498254.2018.1541264 (2019).
10. González-Muñoz, P., Conde-Salazar, L. & Vañó-Galván, S. Allergic contact dermatitis caused by cosmetic products. *Actas Dermosifiliogr.* **9**, 822–32. https://doi.org/10.1016/j.ad.2013.12.018 (2014).
11. Chye, M. et al. Apoptosis induced by para-phenylenediamine involves formation of ROS and activation of p38 and JNK in chang liver cells. *Environ. Toxicol.* **9**, 981–990. https://doi.org/10.1002/tox.21828 (2019).
12. Pot, M., Scheitza, M., Coenraads, J. & Blömeke, B. Penetration and haptenation of p-phenylenediamine. *Contact Dermatitis* **4**, 193–207. https://doi.org/10.1111/cod.12032 (2013).
13. White, M. et al. p-Phenylenediamine allergy: the role of Bandrowski's base. *Clin. Exp. Allergy* **10**, 1289–1293. https://doi.org/10.1111/j.1365-2222.2006.02561.x (2006).
14. Bonifas, J., Scheitza, S., Clemens, J. & Blömeke, B. Characterization of N-acetyltransferase 1 activity in human keratinocytes and modulation by para-phenylenediamine. *J. Pharmacol. Exp. Ther.* **1**, 318–326. https://doi.org/10.1124/jpet.110.167874 (2010).
15. Kawakubo, Y., Merk, F., Masaoudi, A., Sieben, S. & Blömeke, B. N-Acetylation of paraphenylenediamine in human skin and keratinocytes. *J. Pharmacol. Exp. Ther.* **292**(1), 150–155 (2000).

16. Garrigue, L. et al. In vitro genotoxicity of para-phenylenediamine and its N-monoacetyl or N,N'-diacetyl metabolites. *Mutat. Res.* **1**, 58–71. https://doi.org/10.1016/j.mrgentox.2006.05.001 (2006).
17. Mujtaba, S. F. et al. Oxidative-stress-induced cellular toxicity and glycoxidation of biomolecules by cosmetic products under sunlight exposure. *Antioxidants* **10–7**, 1008 (2021).
18. White, J. M. L. et al. p-Phenylenediamine allergy: the role of Bandrowski's base. *Clin. Exp. Allergy* **36**(10), 1289–1293 (2006).
19. Chye, M., Hseu, C., Liang, H., Chen, H. & Chen, C. Single strand dna breaks in human lymphocytes exposed to para-phenylenediamine and its derivatives. *Bull. Environ. Contam. Toxicol.* **1**, 58–62. https://doi.org/10.1007/s00128-007-9316-2 (2008).
20. Onn, C. et al. 4-Chloro-1,2-phenylenediamine induces apoptosis in Mardin-Darby canine kidney cells via activation of caspases. *Environ. Toxicol.* **6**, 655–64. https://doi.org/10.1002/tox.21792 (2014).
21. Wang, S., Mosley, C., Stewart, G. & Yu, H. Photochemical reaction of a dye precursor 4-Chloro-1,2-phenylenediamine and its associated mutagenic effects. *J. Photochem. Photobiol. A Chem.* **1**, 34–39. https://doi.org/10.1016/j.jphotochem.2007.12.002 (2008).
22. Khan, S. et al. 4-Chloro-orthophenylenediamine alters DNA integrity and affects cell survival: inferences from a computational, biophysical/biochemical, microscopic and cell-based study. *J. Biomol. Struct. Dyn.* **11**, 1–12. https://doi.org/10.1080/07391102.2021.2001376 (2021).
23. Warsi, S. et al. 4-Chloro-1,2-phenylenediamine induced structural perturbation and genotoxic aggregation in human serum albumin. *Front. Chem.* **10**, 1016354. https://doi.org/10.3389/fchem.2022.1016354 (2022).
24. Daenen, K. et al. Oxidative stress in chronic kidney disease. *Pediatr. Nephrol.* **6**, 975–991. https://doi.org/10.1007/s00467-018-4005-4 (2019).
25. Oparka, M. et al. Quantifying ROS levels using CM-H_2DCFDA and HyPer. *Methods* **109**, 3–11. https://doi.org/10.1016/j.ymeth.2016.06.008 (2016).
26. Habib, S. & Ali, A. Biochemistry of nitric oxide. *Indian J. Clin. Biochem.* **1**, 3–17. https://doi.org/10.1007/s12291-011-0108-4 (2011).
27. Murata, M., Nishimura, T., Chen, F. & Kawanishi, S. Oxidative DNA damage induced by hair dye components ortho-phenylenediamines and the enhancement by superoxide dismutase. *Mutat. Res.* **2**, 184–191. https://doi.org/10.1016/j.mrgentox.2006.04.014 (2006).
28. Kamiya, H. & Kurokawa, M. Mutagenic bypass of 8-oxo-7,8-dihydroguanine (8-hydroxyguanine) by DNA polymerase κ in human cells. *Chem. Res. Toxicol.* **8**, 1771–1776. https://doi.org/10.1021/tx300259x (2012).
29. Murata, M., Thanan, R., Ma, N. & Kawanishi, S. Role of nitrative and oxidative DNA damage in inflammation-related carcinogenesis. *J. Biomed. Biotechnol.* https://doi.org/10.1155/2012/623019 (2012).
30. El-Haj, L. & Bestle, H. Nitric oxide and sepsis. *Ugeskr Laeger* **44**, V01170086 (2017).
31. Di, C. et al. Application of exhaled nitric oxide (FeNO) in pediatric asthma. *Curr. Opin. Allergy Clin. Immunol.* **2**, 151–158. https://doi.org/10.1097/ACI.0000000000000726 (2021).
32. Konstantinova, T. S. et al. Modification of the nitric oxide concentration regulates the development of the apoptosis in the eye retina. *Biofizika* **2**, 325–30 (2012).
33. Murata, M. Inflammation and cancer. *Environ. Health Prev. Med.* **1**, 50. https://doi.org/10.1186/s12199-018-0740-1.PMID:30340457;PMCID:PMC6195709 (2018).
34. Verigos, E., Sagredou, S., Orfanakos, K., Dalezis, P. & Trafalis, T. 8-hydroxy-2'-deoxyguanosine and 8-nitroguanine production and detection in blood serum of breast cancer patients in response to postoperative complementary external ionizing irradiation of normal tissues. *Dose Response* **4**, 1559325820982172. https://doi.org/10.1177/1559325820982172. (2020).
35. Ohshima, H., Sawa, T. & Akaike, T. 8-nitroguanine, a product of nitrative DNA damage caused by reactive nitrogen species: formation, occurrence, and implications in inflammation and carcinogenesis. *Antioxid. Redox Signal.* **5–6**, 1033–1034. https://doi.org/10.1089/ars.2006.8.1033 (2006).
36. Yermilov, V., Rubio, J. & Ohshima, H. Formation of 8-nitroguanine in DNA treated with peroxynitrite in vitro and its rapid removal from DNA by depurination. *FEBS Lett.* **3**, 207–210. https://doi.org/10.1016/0014-5793(95)01281-6 (1995).
37. Warsi, S. et al. Characterization of human serum albumin modified by hair dye component, 4-Chloro-1,2-phenylenediamine: Role in protein aggregation, redox biology and cytotoxicity. *J. Mol. Liq.* **331**, 115731 (2021).
38. Coogan, P. F. et al. Hair product use and breast cancer incidence in the Black Women's Health Study. *Carcinogenesis* **7**, 924–930. https://doi.org/10.1093/carcin/bgab041 (2021).
39. Cook, L. S., Malone, K. E., Daling, J. R., Voigt, L. F. & Weiss, N. S. Hair product use and the risk of breast cancer in young women. *Cancer Causes Control.* **6**, 551–9. https://doi.org/10.1023/a:1008903126798 (1999).
40. Ahmadi, M. et al. Association between hair dye use and cancer in women: a systematic review and meta-analysis of case-control studies. *Afr. Health Sci.* **2**, 323–333. https://doi.org/10.4314/ahs.v22i2.36 (2022).
41. Turati, F., Pelucchi, C., Galeone, C., Decarli, A. & La Vecchia, C. Personal hair dye use and bladder cancer: a meta-analysis. *Ann. Epidemiol.* **2**, 151–9. https://doi.org/10.1016/j.annepidem.2013.11.003 (2014).
42. Chang, C. J. et al. Use of straighteners and other hair products and incident uterine cancer. *J. Natl. Cancer Inst.* **12**, 1636–1645. https://doi.org/10.1093/jnci/djac165 (2022).
43. Zhang, Y., Kim, C. & Zheng, T. Hair dye use and risk of human cancer. *Front. Biosci. (Elite Ed.)* **1**, 516–528. https://doi.org/10.2741/397 (2012).
44. Kashfi, K. Nitric oxide in cancer and beyond. *Biochem. Pharmacol.* **176**, 114006. https://doi.org/10.1016/j.bcp.2020.114006 (2020).
45. Guzik, T. J., Korbut, R. & Adamek-Guzik, T. Nitric oxide and superoxide in inflammation and immune regulation. *J. Physiol. Pharmacol.* **4**, 469–87 (2003).
46. Kay, J., Thadhani, E., Samson, L. & Engelward, B. Inflammation-induced DNA damage, mutations and cancer. *DNA Repair (Amst.)* **83**, 102673. https://doi.org/10.1016/j.dnarep.2019.102673 (2019).
47. Förstermann, U. & Sessa, W. C. Nitric oxide synthases: regulation and function. *Eur. Heart J.* **7**(829–37), 837a–837d. https://doi.org/10.1093/eurheartj/ehr304 (2012).
48. Al-Shehri, S. S. Reactive oxygen and nitrogen species and innate immune response. *Biochimie* **181**, 52–64. https://doi.org/10.1016/j.biochi.2020.11.022 (2021).
49. Lushchak, V. I. & Lushchak, O. Interplay between reactive oxygen and nitrogen species in living organisms. *Chem. Biol. Interact.* **349**, 109680. https://doi.org/10.1016/j.cbi.2021.109680 (2021).
50. Ahmad, R., Hussain, A. & Ahsan, H. Peroxynitrite: cellular pathology and implications in autoimmunity. *J. Immunoassay Immunochem.* **2**, 123–138. https://doi.org/10.1080/15321819.2019.1583109 (2019).
51. Pisoschi, A. M. & Pop, A. The role of antioxidants in the chemistry of oxidative stress: A review. *Eur. J. Med. Chem.* **97**, 55–74. https://doi.org/10.1016/j.ejmech.2015.04.040 (2015).
52. Pacher, P., Beckman, J. S. & Liaudet, L. Nitric oxide and peroxynitrite in health and disease. *Physiol. Rev.* **1**, 315–424. https://doi.org/10.1152/physrev.00029.2006 (2007).
53. Basu, A. K. DNA damage, mutagenesis and cancer. *Int. J. Mol. Sci.* **4**, 970. https://doi.org/10.3390/ijms19040970 (2018).
54. Caliri, A. W., Tommasi, S. & Besaratinia, A. Relationships among smoking, oxidative stress, inflammation, macromolecular damage, and cancer. *Mutat. Res. Rev. Mutat. Res.* **787**, 108365. https://doi.org/10.1016/j.mrrev.2021.108365 (2021).
55. Valko, M., Rhodes, C. J., Moncol, J., Izakovic, M. & Mazur, M. Free radicals, metals and antioxidants in oxidative stress-induced cancer. *Chem. Biol. Interact.* **1**, 1–40. https://doi.org/10.1016/j.cbi.2005.12.009 (2006).
56. Jelic, M. D., Mandic, A. D., Maricic, S. M. & Srdjenovic, B. U. Oxidative stress and its role in cancer. *J. Cancer Res. Ther.* **1**, 22–28. https://doi.org/10.4103/jcrt.JCRT_862_16 (2021).

57. Tantry, I. Q. et al. Hypochlorous acid induced structural and conformational modifications in human DNA: A multi-spectroscopic study. *Int. J. Biol. Macromol.* **106**, 551–558. https://doi.org/10.1016/j.ijbiomac.2017.08.051 (2018).
58. Tripathi, P. et al. Peroxynitrite modified DNA presents better epitopes for anti-DNA autoantibodies in diabetes type 1 patients. *Cell. Immunol.* **1**, 30–38. https://doi.org/10.1016/j.cellimm.2014.04.012 (2014).
59. Ahn, Y. Y., Kim, J. & Kim, K. Frozen hydrogen peroxide and nitrite solution: The acceleration of benzoic acid oxidation via the decreased pH in ice. *Environ. Sci Technol.* **4**, 2323–2333. https://doi.org/10.1021/acs.est.1c05705 (2022).
60. Robinson, K. M. & Beckman, J. S. Synthesis of peroxynitrite from nitrite and hydrogen peroxide. *Methods Enzymol.* **396**, 207–14. https://doi.org/10.1016/S0076-6879(05)96019-9 (2005).
61. Rosu, F. et al. UV spectroscopy of DNA duplex and quadruplex structures in the gas phase. *J. Phys. Chem. A* **22**, 5383–5391. https://doi.org/10.1021/jp302468x (2012).
62. Hu, Y., Xie, M. & Wu, X. Interaction studies of sodium cyclamate with DNA revealed by spectroscopy methods. *Spectrochim. Acta A Mol. Biomol. Spectrosc.* **220**, 117085. https://doi.org/10.1016/j.saa.2019.04.077 (2019).
63. Green, M. R. & Sambrook, J. Mapping RNA with Nuclease S1. *Cold Spring Harb. Protoc.* https://doi.org/10.1101/pdb.prot101824 (2021).
64. He, L., Michailidou, F., Gahlon, H. L. & Zeng, W. Hair dye ingredients and potential health risks from exposure to hair dyeing. *Chem. Res. Toxicol.* **6**, 901–915. https://doi.org/10.1021/acs.chemrestox.1c00427 (2022).
65. Zhan, X., Huang, Y. & Qian, S. Protein tyrosine nitration in lung cancer: Current research status and future perspectives. *Curr. Med. Chem.* **29**, 3435–3454. https://doi.org/10.2174/0929867325666180221140745 (2018).
66. Saito, S. T., Silva, G., Pungartnik, C. & Brendel, M. Study of DNA-emodin interaction by FTIR and UV-vis spectroscopy. *J. Photochem. Photobiol. B* **111**, 59–63. https://doi.org/10.1016/j.jphotobiol.2012.03.012 (2012).
67. Mustafa, M. et al. Biophysical characterization of structural and conformational changes in methylmethane sulfonate modified DNA leading to the frizzled backbone structure and strand breaks in DNA. *J. Biomol. Struct. Dyn.* **16**, 7598–7611. https://doi.org/10.1080/07391102.2021.1899051 (2022).
68. Chepelev, N. L. et al. HPLC measurement of the DNA oxidation biomarker, 8-oxo-7,8-dihydro-2'-deoxyguanosine, in cultured cells and animal tissues. *J. Vis. Exp.* **102**, e52697. https://doi.org/10.3791/52697.PMID:26273842;PMCID:PMC4544582 (2015).
69. Chang, H. R., Lai, C. C., Lian, J. D., Lin, C. C. & Wang, C. J. Formation of 8-nitroguanine in blood of patients with inflammatory gouty arthritis. *Clin. Chim. Acta* **1–2**, 170–5. https://doi.org/10.1016/j.cccn.2005.06.003 (2005).
70. Hiraku, Y. & Kawanishi, S. Immunohistochemical analysis of 8-nitroguanine, a nitrative DNA lesion, in relation to inflammation-associated carcinogenesis. *Methods Mol. Biol.* **512**, 3–13. https://doi.org/10.1007/978-1-60327-530-9_1 (2009).
71. Ma, Q. Role of nrf2 in oxidative stress and toxicity. *Annu. Rev. Pharmacol. Toxicol.* **53**, 401–426. https://doi.org/10.1146/annurev-pharmtox-011112-140320 (2013).
72. Ersoy, Y. et al. Serum nitrate and nitrite levels in patients with rheumatoid arthritis, ankylosing spondylitis, and osteoarthritis. *Ann. Rheum. Dis.* **61**(1), 76–78 (2002).
73. Manwaring, J. et al. Extrapolation of systemic bioavailability assessing skin absorption and epidermal and hepatic metabolism of aromatic amine hair dyes in vitro. *Toxicol. Appl. Pharmacol.* **2**, 139–148. https://doi.org/10.1016/j.taap.2015.05.016 (2015).
74. Zanoni, T. B. et al. The oxidation of p-phenylenediamine, an ingredient used for permanent hair dyeing purposes, leads to the formation of hydroxyl radicals: Oxidative stress and DNA damage in human immortalized keratinocytes. *Toxicol. Lett.* **3**, 194–204. https://doi.org/10.1016/j.toxlet.2015.09.026 (2015).
75. Habib, S., Moinuddin, Ali, A. & Ali, R. Preferential recognition of peroxynitrite modified human DNA by circulating autoantibodies in cancer patients. *Cell Immunol.* **2**, 117–23. https://doi.org/10.1016/j.cellimm.2008.08.002 (2009).
76. Reuter, S., Gupta, S. C., Chaturvedi, M. M. & Aggarwal, B. B. Oxidative stress, inflammation, and cancer: how are they linked?. *Free Radic. Biol. Med.* **11**, 1603–16. https://doi.org/10.1016/j.freeradbiomed.2010.09.006 (2010).
77. Klaunig, J. E. Oxidative stress and cancer. *Curr. Pharm. Des.* **40**, 4771–4778. https://doi.org/10.2174/1381612825666190215121712 (2018).
78. Waris, S. et al. Molecular docking explores heightened immunogenicity and structural dynamics of acetaldehyde human immunoglobulin G adduct. *IUBMB Life* **10**, 1522–1536. https://doi.org/10.1002/iub.2078 (2019).
79. Habib, S., Moinuddin, & Ali, R. Peroxynitrite-modified DNA: a better antigen for systemic lupus erythematosus anti-DNA autoantibodies. *Biotechnol. Appl. Biochem.* **2**, 65–70. https://doi.org/10.1042/BA20050156 (2006).
80. Agita, A. & Alsagaff, M. T. Inflammation, Immunity, and Hypertension. *Acta Med. Indones.* **2**, 158–165 (2017).
81. Raza, A. et al. Fructosylation of human insulin causes AGEs formation, structural perturbations and morphological changes: an in silico and multispectroscopic study. *J. Biomol. Struct. Dyn.* **41**(12), 5850–5862. https://doi.org/10.1080/07391102.2022.2098820 (2023).
82. Ishikawa, R. et al. Stabilization of telomeric G-quadruplex by ligand binding increases susceptibility to S1 nuclease. *Chem. Commun. (Camb.)* **59**, 7236–7239. https://doi.org/10.1039/D1CC03294A (2021).
83. Voytas, D. Agarose gel electrophoresis. *Curr. Protoc. Mol. Biol.* https://doi.org/10.1002/0471142727.mb0205as51 (2001).
84. Gomes, R. et al. FTIR spectroscopy with machine learning: A new approach to animal DNA polymorphism screening. *Spectrochim. Acta A Mol. Biomol. Spectrosc.* **261**, 120036. https://doi.org/10.1016/j.saa.2021.120036 (2021).
85. Hassan, A., Macedo, L. J. A., Souza, J. C. P., Lima, F. C. D. A. & Crespilho, F. N. A combined Far-FTIR, FTIR spectromicroscopy, and DFT study of the effect of DNA binding on the [4Fe4S] cluster site in EndoIII. *Sci. Rep.* **1**, 1931. https://doi.org/10.1038/s41598-020-58531-4 (2020).
86. Cadet, J. et al. Assessment of oxidative base damage to isolated and cellular DNA by HPLC-MS/MS measurement. *Free Radic. Biol. Med.* **4**, 441–9. https://doi.org/10.1016/s0891-5849(02)00820-1 (2002).
87. Chepelev, N. L. et al. HPLC measurement of the DNA oxidation biomarker, 8-oxo-7,8-dihydro-2'-deoxyguanosine, in cultured cells and animal tissues. *J. Vis. Exp.* **1**(102), e52697. https://doi.org/10.3791/52697 (2015).
88. Lee, Y. J. & Weigele, P. R. Detection of modified bases in bacteriophage genomic DNA. *Methods Mol. Biol.* **198**, 53–66. https://doi.org/10.1007/978-1-0716-0876-0_5 (2021).
89. Vargas-Maya, N. I. Refinement of the Griess method for measuring nitrite in biological samples. *J. Microbiol. Methods* **187**, 106260. https://doi.org/10.1016/j.mimet.2021.106260 (2021).
90. Tsikas, D. Analysis of nitrite and nitrate in biological fluids by assays based on the Griess reaction: appraisal of the Griess reaction in the L-arginine/nitric oxide area of research. *J. Chromatogr. B Analyt. Technol. Biomed. Life Sci.* **1–2**, 51–70. https://doi.org/10.1016/j.jchromb.2006.07.054 (2007).
91. Giustarini, D., Rossi, R., Milzani, A. & Dalle-Donne, I. Nitrite and nitrate measurement by Griess reagent in human plasma: evaluation of interferences and standardization. *Methods Enzymol.* **440**, 361–380. https://doi.org/10.1016/S0076-6879(07)00823-3 (2008).
92. Ali, R. & Alam, K. Evaluation of antibodies against oxygen free radical-modified DNA by ELISA. *Methods Mol. Biol.* **186**, 171–181. https://doi.org/10.1385/1-59259-173-6:171 (2002).
93. Ota, S., Yui, Y., Sato, T., Yoshimoto, N. & Yamamoto, S. Rapid purification of immunoglobulin G using a protein A- immobilized monolithic spin column with hydrophilic polymers. *Anal. Sci.* **7**, 985–990. https://doi.org/10.2116/analsci.20P378 (2021).
94. Hober, S., Nord, K. & Linhult, M. Protein A chromatography for antibody purification. *J. Chromatogr. B Analyt. Technol. Biomed. Life Sci.* **1**, 40–47. https://doi.org/10.1016/j.jchromb.2006.09.030 (2007).
95. Keyhani, J. & Keyhani, E. Detection of DNA autoantibodies by electrophoretic mobility shift assay. *Methods Mol. Biol.* **1901**, 133–152. https://doi.org/10.1007/978-1-4939-8949-2_11 (2019).

96. Hellman, L. M. & Fried, M. G. Electrophoretic mobility shift assay (EMSA) for detecting protein-nucleic acid interactions. *Nat. Protoc.* **8**, 1849–61. https://doi.org/10.1038/nprot.2007.249 (2007).

Acknowledgements
The support of the University Sophisticated Instrumentation Facility (USIF), AMU, Aligarh is duly acknowledged.

Author contributions
SK: conceptualization, methodology, experimentation, validation, original draft preparation; AA: supervision, conceptualization, validation, reviewing; MSW: resources, reviewing, proof-reading; SW: reviewing, experimental analysis; AR: editing; SAA: resources; MM: reviewing; MU: experimental analysis, editing; SAS: resources, formal analysis; RM: editing, reviewing; SH: conceptualization, resources, supervision, visualization, original draft preparation, reviewing, editing.

Declarations

Competing interests
The authors declare no competing interests.

Additional information
Supplementary Information The online version contains supplementary material available at https://doi.org/10.1038/s41598-024-75649-x.

Correspondence and requests for materials should be addressed to S.H.